Signature Simulation of Mixed Materials

Tyler D. Carson[a] and Carl Salvaggio[a]
[a]Rochester Institute of Technology, Chester F. Carlson Center for Imaging Science, 54 Lomb Memorial Drive, Rochester, NY, USA 14623

ABSTRACT

Soil target signatures vary due to geometry, chemical composition, and scene radiometry. Although radiative transfer models and function-fit physical models may describe certain targets in limited depth, the ability to incorporate all three signature variables is difficult. This work describes a method to simulate the transient signatures of soil by first considering scene geometry synthetically created using 3D physics engines. Through the assignment of spectral data from the Nonconventional Exploitation Factors Data System (NEFDS), the synthetic scene is represented as a physical mixture of particles. Finally, first principles radiometry is modeled using the Digital Imaging and Remote Sensing Image Generation (DIRSIG) model. With DIRSIG, radiometric and sensing conditions were systematically manipulated to produce and record goniometric signatures. The implementation of this virtual goniometer allows users to examine how a target bidirectional reflectance distribution function (BRDF) will change with geometry, composition, and illumination direction. By using 3D computer graphics models, this process does not require geometric assumptions that are native to many radiative transfer models. It delivers a discrete method to circumnavigate the significant cost of time and treasure associated with hardware-based goniometric data collections.

Keywords: BRDF, DIRSIG, goniometer, NEFDS

1. INTRODUCTION

How can we pinpoint the directional scattering of colored light from surfaces comprised of mixed materials? Surface properties of reflectance and emissivity are parameters required to define a scattering signature. Many specimens in our world are made of material mixtures. Consequently, optical properties that describe surface radiometry can vary within a single target.

At first thought, making goniometric measurements might seem like the best and only method to define the reflective features of solid material mixtures.[1-3] Logistically, it is a difficult solution. A robust target signature would require measurements at every view angle, lighting scenario, and mixture composition. To ensure consistent measurements that can be compared with observations of other targets and scenes, the same sensor or sensor characteristics should be used for each goniometric measurement. The optical and radiometric characteristics of the imaging system should be repeatable. In situ target geometry for many surfaces is also difficult or impossible to replicate in lab environments.[4] Traveling to targets of interest is often costly and is always weather dependent. Therefore, a physic-based signature creation tool would be of great value. Simulation experiments could be completed rapidly, and modified in a physical fashion. The basis of such a modeling tool lies in the realm of computer graphics. Accurate measurements require precise virtual geometry, goniometric measurement, and evaluation tools that plausibly describe nature. These deliverables have their origin in the form of procedural shaders used by artists. A shader is simply an algorithm that produces the physically possible or visually pleasing levels of light and color in an image.

To truly mimic reality, lighting and shading should be consistent for all scenes and materials. Pre-existing material reflectance databases[5] have been exploited in order to test new algorithms.[6] Algorithm designers wish to find or create models that are physically based, while still providing adjustable parameters for artistic control or data fitting. Many published models have been refined over time to include comprehensive physical traits such as index of refraction or faceted surfaces.[7, 8] A problem for both animators and scientists alike, is the narrow scope of most models. Accuracy is sacrificed in exchange for concise comprehensive equations that can be used for many different material surfaces. Certain pure materials have been characterized quite well by functional data fit models.[9-13] However, a single descriptor for all material compositions has yet to be derived. Variance in reflection is precisely why graphic artists and scientists need a test-bed to define materials and models that describe them. Developing such a tool will exhibit shortcomings,

Radar Sensor Technology XIX; and Active and Passive Signatures VI, edited by G. Charmaine Gilbreath
Kenneth I. Ranney, Chadwick Todd Hawley, Armin Doerry, Proc. of SPIE Vol. 9461, 94611J
 · doi: 10.1117/12.2176990

advantages, and limits of simulation.

The Rochester Institute of Technology (RIT) has developed tools to aid in the exploration of non-uniform directional reflectance.[14-16] Digital Imaging and Remote Sensing Image Generation (DIRSIG) provides a supplemental work-around for many of the problems and inaccuracies inherent to data collects. DIRSIG is a radiometry model that tracks the radiation of light between a user-defined source, target, and sensor. With this tool, unique lighting and sensing scenarios can be studied in depth using a multitude of different user-created targets. DIRSIG does not require surfaces to be described by a mathematical form. Surfaces can be created using graphic modeling tools.[14] In order to produce a simulated synthetic output image of a sensor, the solid angle of a detector is tracked as rays of light bounce between materials that make up a surface. With user manipulation, a single simulation can capture directional reflectance at all angles in the hemisphere above a target. Specifically, a full hemispherical bidirectional reflectance distribution function (BRDF)[17] could be created for any angular resolution of zenith and azimuth angles.

The study of the reflectance of soil is especially relevant to modeling and simulation because the physics of solids are well understood. Bänninger[18] and others[19, 20] built upon earlier work of soil specific radiative transfer[13] to link the spatial characteristics of mixed soils to BRDF. By treating particles as layered thin films, subsurface soil scattering was determined by the thickness and refractive index of each thin slab. This work connected light scatter to surface texture. Based on the evaluation of graphic shaders, one would expect texture and backscatter effects to be noticeable at large zenith angles. Bänninger showed that the influence of texture on reflectance is measureable at zenith angles as small as 45 degrees. Using polarization effects, investigations[20] also confirmed an increase in reflectance and decrease in transmittance with decreasing particle size. The model by Li[19] correctly predicted the tinted appearance of rough soil surfaces that is brought on by shadowing and multiple top-surface reflections.

Wang[1] attempted to gain insight into soil reflectance through the use of advanced imaging spectrometers oriented in multiple view directions. Such tools were also used by Kerekes[21] to make reflectance and emissivity measurements of contaminated surfaces. It was shown that rougher surfaces exhibit greater variation in BRDF than do smooth surfaces. Also, variation in BRDF generated from 800nm-2,000nm light sources is more distinct than those generated from visible illumination. This supports the use of BRDF for target identification.

The following sections describe a new goniometric tool that serves as a test-bed for the signatures of mixed solids in the optical and near-infrared (NIR) wavelength regimes. The research has three main components: a virtual goniometer structure, a method to realistically create mixed solids on the particle scale, and a simulation tool to apply realistic lighting and material properties. The paper concludes with comparisons between the virtual goniometer data and directional reflectance physically acquired in a laboratory[1].

2. METHODOLOGY

Material definition hinges upon the understanding of the radiation signal that propagates between a material and a sensor. Radiance that reaches the entrance pupil of a sensor is dependent upon the reflectance distribution and can be written as

$$L(\lambda,\theta_v,\phi_v,\theta_l,\phi_l) = \left[\frac{E_l(\lambda)}{\pi}\cos(\theta_l)\,\tau_1(\lambda,\theta_l)\rho(\lambda,\theta_v,\phi_v,\theta_l,\phi_l) + \epsilon(\lambda,\theta_v,\phi_v)L_T\right]\tau_2(\lambda,\theta_v) + L_u(\lambda,\theta_v) \quad (1)$$

The angular orientation of the solar light source is represented with (θ_l,ϕ_l), while the sensor viewing position is described using (θ_v,ϕ_v). E_l defines radiation that is emitted from a single light source. The spectral bidirectional reflectance function $\rho\,(\lambda,\theta_v,\phi_v,\theta_l,\phi_l)$ depends on the directionality of both the sensor and the light source. As this governing equation is wavelength dependent, self-emitted blackbody radiance $L_T\,(\lambda,T)$ and directional emissivity $\epsilon\,(\lambda,\theta_v,\phi_v)$ are also considered in the calculation of sensor reaching radiance. Transmission of radiation is denoted by τ. Additional upwelling path radiance is represented as L_u.

The bidirectional reflectance function serves as a distinctive signature of target geometry and chemical composition. BRDF has units of inverse steradians, and is defined as the ratio of radiance leaving a surface to the irradiance that is incident upon that same surface.

$$\rho_{BRDF}(\lambda, \theta_v, \phi_v, \theta_l, \phi_l) = L(\lambda, \theta_r, \phi_r)/E(\lambda, \theta_i, \phi_i)\,[sr^{-1}] \quad (2)$$

In order to simulate BRDF, the target geometry, surface composition and scene radiometry must each be carefully considered.

2.1 Target Geometry Construction

Creating accurate models of nature requires very good synthetic scene generation. Many computer-aided design (CAD) softwares give users the ability to etch, bend, and connect different shapes or planes to create objects with precision. Entire target scenes can be created by deliberately placing CAD objects within a virtual three-dimensional space in an attempt to mimic reality.

For example, creating a scene of sand or soil might require the design of several different particles that are cloned, rotated, and individually placed with respect to one another in the form of a sand pile. A sand scene might be comprised of thousands of objects. Placing each object individually would be incredibly tedious and time consuming. Even if users had the ability to place the objects quickly, could they be posed in a physical fashion that realistically represents nature? Using the Blender 3D open source software and its physics engine, one can create a scene of objects that interact based on the physical properties assigned by the user. Simulating rigid body collisions, fluid motion, and force field interactions are all possible using the Blender 3D tool. Individual mesh objects are subject to friction and damping and also interact through collisions based on mass.

One additional feature that makes Blender 3D a great tool for creating geometry with which one can model reflectance is the ability to match the shape of each rigid body object to its own mesh geometry within a physics simulation. This means that collisions between objects are influenced by every facet of each object, rather than representing the physical bounds of a mesh with a convex hull. For instance, a multi-faceted particle is bounded in the Blender 3D physics engine as a multi-faceted object rather than a six-sided cube with similar volume (see Figure 1).

A study by Wang[1] and the University of Lethbridge aimed to characterize the directional reflectance of soils using a goniometric imaging spectrometer. Using Blender 3D, an attempt was made to replicate this target surface. Soil is granular in nature, and a synthetic target should represent this prevalent characteristic. In this study, the Blender 3D physics engine was used to mix and naturally pose particulates within the scene. Particles are not individually placed by hand. They are treated as rigid bodies and are dropped onto a surface where they interact with each other and the surface itself. This creates a 3D scene, shown in Figure 1, that is more physical than those used in the derivation of many well-known reflectance functions.[5,7,9,13]

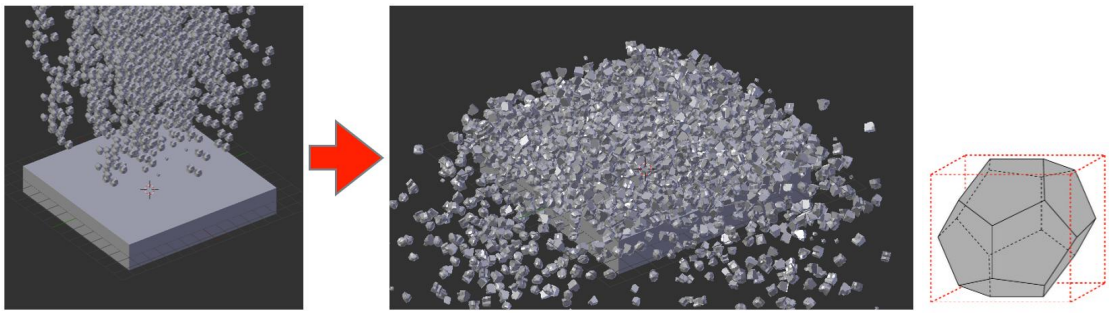

Figure 1. Using the Blender 3D physics engine, particles can be dropped as rigid bodies. They interact and settle naturally in space. This process is represented as a motion picture. Single motion picture frames can be extracted and used as a target scene. [http://www.cis.rit.edu/~cnspci/media/publications/video/spie9461-62_figure1.php]

The soil scene simulation shown above is a frame from a motion picture depicting particle interactions. At each frame, particle position is calculated using the mass, shape, and external forces preprogrammed into the physics engine. A single frame is used to create a scene for radiometry simulation. Motion picture frames are exported from Blender 3D as object database (OBJ) files. These files include the numerical geometry that defines a scene. This includes the position in

x,y,z coordinates of all object vertices. Object faces are defined as a collection of numbered vertices. The name of the material assigned to each face is also exported within the OBJ file.

Soil particulates shown in Figure 1 range in diameter from 0.320 mm to 2mm. Particles of four different sizes (0.320mm, 0.640mm, 1.28mm and 2mm) were used for the virtual construction of the scene. These four evenly distributed geometries were replicated many times to create a scene with greater than seven thousand particles. Twenty-five instances of the scene were tiled together to create the final soil scene that was used as a target for the DIRSIG-based goniometer.

2.2 Surface Composition

The optical properties of targets used in conjunction with DIRSIG are obtained from databases of materials. The reflectance information from a database is applied individually to facets in a synthetic scene to produce radiometric ray-trace results that are consistent with each material being modeled. Directional hemispherical reflectance (DHR) signatures for many pure targets have been collected by Rochester Institute of Technology (RIT) and the United States Geological Survey (USGS) (http://speclab.cr.usgs.gov). Reflectance spectra for the sand particles created for this simulation were found in the USGS database. Each individual facet of a Blender 3D-generated object can be assigned with spectral properties from any of these libraries. A goal of this research is to characterize mixed materials. By mixing facetized objects that have been assigned specific optical characteristics, mixed material spectra can be created. These material descriptors require DHR data to describe diffuse materials (soils) and directional reflectance data to define specular materials (painted metals).

Another deep library that includes BRDF signatures of many materials is the Nonconventional Exploitation Factors Data System (NEFDS). The NEFDS provides a standardized database of reflectance information. To obtain this data, the National Geospatial-Intelligence Agency (NGA) has selected and examined twelve target categories containing more than 400 different materials and mixtures. Each material in the database has been measured goniometrically using precisely calibrated sensors and experimental procedures. Laser polarization measurements in the specular and backscatter direction provide data that can be used to tease out descriptions of specular, diffuse and volumetric scatter. Using the Beard-Maxwell[22] BRDF model paired with these measured data points, regression is performed to find the optimal reflectance coefficient for each view angle at every illumination position. Because there are a large number of free parameters in this BRDF, and these parameters correspond to physical material properties, NEFDS parameters tend to closely mimic experimental observations. The actual NEF product is a list of BRDF parameters for each specific measurement of each target in the database. NEFDS measurements are performed at multiple wavelengths, providing a measuring stick for wavelength dependent results produced using synthetic DIRSIG scenes.

For materials that are characterized by strong specular scattering, the directional reflectance measurements provided by the NEFDS are especially important. Since measurements by Kerekes[21] investigated the spectral signatures of soiled automobiles, the following model includes a target of soil contaminated car paint. Directional reflectance was not measured by Kerekes, therefore the surrogate reflectance properties of blue colored car paint were mined from the NEFDS.

2.3 Goniometric Radiance Generation of a Synthetic Scene using DIRSIG

Scenes developed using the aforementioned Blender 3D tool can be thought of as a superposition of flat facets. Using the Digital Imaging and Remote Sensing Image Generation (DIRSIG) tool, computational radiometry is applied to each facet in a scene through ray tracing. This allows for the construction of models from first principles through the numerical assembly of facets. DIRSIG models consider the atmosphere, environment, illumination, observation geometry, and interactions between facets. Each of these scene parameters is designed and defined by the user. The output of any DIRSIG simulation is a synthetic image corresponding to signal from wavelengths in the visible spectrum through the thermal infrared. The signal at each pixel in the image corresponds to radiance detected by the DIRSIG sensor. Target reflectance can be calculated from this data.

DIRSIG images are dependent upon user-selected sub-models. Such inputs might include reflectance properties to be assigned to facets or atmospheric data, which may modify the intensity of light reaching the DIRSIG sensor. Cameras

can also be created and modified virtually within the DIRSIG environment. Users must also select parameters of solar position and target view angle in order to initialize ray tracing and data collection. Each preset parameter is gathered and correctly executed through the use of a simulation file.

The compartmentalization of DIRSIG data inputs allow for remote sensing experimentation. This research includes the analysis of novel DIRSIG scenes using standardized radiometry and material properties. Because DIRSIG considers mesh objects on the scale of facets, different material properties can be individually assigned to every facet in the scene. Why is this important? With the ability to make individual reflectance assignments, scenes of mixed solids and contaminated surfaces can be modeled with respect to radiometry and geometry. For example, the surface presented in Figure 2 could be attributed with the optical properties of blue car paint, while the soil particles that cover the surface are given the spectral signature of pure sand.

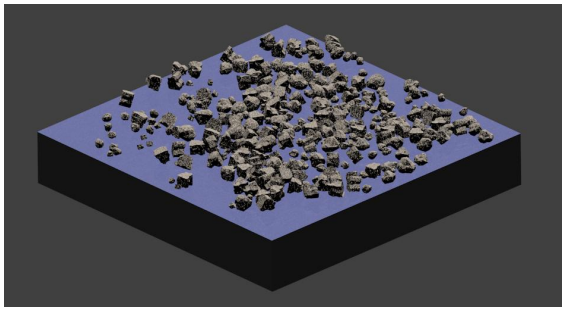

Figure 2. Using Blender 3D and DIRSIG, a mixed target of blue car paint and soil can be created.

In order to perform BRDF and directional emissivity analysis on virtual scenes, a virtual goniometer can be developed in DIRSIG. Ideally, all iterative hemispherical measurements should be performed and analyzed upon the execution of a single file. The construction of this file is the subject of this section. It includes the DIRSIG simulation file, shell file construction, Python editing, and ENVI file analysis. The workflow for this process is displayed in Figure 3.

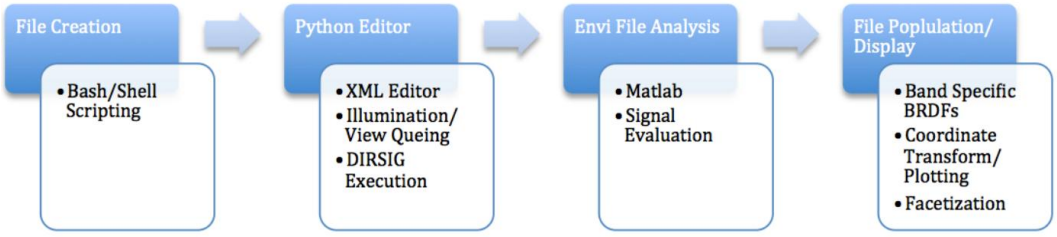

Figure 3. The workflow for this virtual goniometer includes shell executable file. Within this file, DIRSIG parameters are edited using an XML file editor and simulated radiance data is analyzed automatically with MATLAB.

The shell file, as seen in Figure 3, allows a user to define parameters of a DIRSIG scene and execute a radiometric ray trace. This file takes the form of a bash script and initiates the execution of goniometric measurements. It can be executed from the command line and has four functions.

First, the script opens MATLAB and initializes an output text file that will be used for analysis. This text file is a placeholder for output radiance and wavelength values. It is initially left blank.

Next, the code allows the goniometer parameters to be set from the command line. These parameters are necessary DIRSIG inputs. They include the distance between the ground and imaging system, the angular resolution of the goniometer in azimuth and zenith, the position of the solar source, the total irradiance (W/cm^2) emanating from the source, the balance between direct source illumination and hemispherical illumination, and the name of the scene

geometry file that will be subjected to the radiometry.

Third, a Python script executes DIRSIG simulation files. A full hemispherical goniometer measurement could require more than one hundred DIRSIG simulation runs. For each run, Extensible Markup Files (XML) files are modified to provide scene, atmospheric, sensor and tasking information. The creation of all of these files is tedious and inflexible. Without the scripted Python editor, a change to the imaging platform focal length would require the user to edit an XML file for every simulation file in the batch. This might require more than one hundred simulation files to be handled individually. The Python XML editor provides a process for editing a single simulation file rather than hundreds. MATLAB is then triggered once again to calculate average radiance from the DIRSIG output, ENVI formatted image files. It then appends the radiance and corresponding wavelength data to the output file created in the first step. With sensor reaching radiance in hand, BRDF can be calculated using Equation 2.

In summary, this script describes and executes each step of the virtual goniometric measurement.

2.4 Virtual Goniometer Construction

To validate this study, the DIRSIG goniometer that is presented above was built as a replica of a hardware system used by the University of Lethbridge in Alberta, Canada[1]. In their experiment, and in ours, a 35mm focal length camera was used at a hemispherical measurement distance of 1780mm. The imaging system was sensitive to wavelengths between 400 and 700nm with a spectral resolution of 0.5nm. Distinct spectral bands were represented as Gaussian responsivity functions at 450, 550 and 650nm. At an observation distance of 1.780m, the Hamamatsu C8484-05G imaging spectrometer used by Wang[1] has a field of view (FOV) of 0.88m in the x-axis and 0.67m in the y-axis, 140 pixels in each spatial dimension from the center of the FOV were used for BRDF analysis in that study. This is necessary since each image in a goniometric measurement contains the same target; and at large declination angles, an imager will observe portions of the background that are not sensed at viewing positions near nadir. The consequence of using a 140^2 pixel area for analysis is a reduced nadir FOV of 91.84mm. The 140^2 pixel configuration was mimicked in our virtual experiment. The light source in both the physical experiment and the virtual experiment was placed at a zenith/declination angle of $30°$ from nadir. In the virtual experiment, light was modeled as a point source. This layout is a close approximation to the halogen light source used in the laboratory at the University of Lethbridge.

The virtual hardware was set to take measurements at view zenith angles between $0°$ and $80°$ and azimuth angles over the full $360°$. Angular resolution of $20°$ was used for both the zenith and azimuthal dimensions. The target was illuminated by a static source that remained in the same $30°$ zenith position throughout the goniometric data acquisition.

After data was collected for every view location, average sensor reaching radiance was used in conjunction with Equation 2 to find BRDF for each spectral band. This can be solved without using a calibration panel (as was done by Wang[1]) because the irradiance ($E(\lambda, \theta_i, \phi_i)$) that is incident upon the virtual target is completely defined by the DIRSIG user.

2.5 Goniometric Modeling using the NEFDS

Soil often contaminates specular man-made targets. These targets will be misrepresented by a sensor in DIRSIG if inappropriate material optical properties are assigned to the objects being mixed. For targets with a specular quality, actual reflectance is large in certain view directions and smaller in others. In order to model the reflectance variability properly, DIRSIG requires directional reflectance information. The Non-conventional Exploitation Factors Data System (NEFDS) was detailed in Section 2.2. It is a standardized database of directional reflectance information. It contains data for many man-made materials, including car paints.

The blue painted virtual surface used in this work was attributed with a full BRDF material file from the NEFDS. This means that when a DIRSIG sensor views the painted target from the specular direction it will detect a very high level of radiance. Likewise, a DIRSIG sensor situated at an azimuth angle that is perpendicular to the specular plane of the car paint will observe much less radiance because car paint is a very specular material. The soil particles used as contaminants in this study were assigned with a directional hemispherical reflectance (DHR) file from the USGS. Without the geometric complexity created in Blender 3-D, a plane assigned with the soil DHR would possess the same

level of reflectance in both the specular and perpendicular viewing locations. The remainder of this paper reveals that Blender 3-D particle geometry coupled with DIRSIG can simulate directional reflectance of soil contamination.

A study was formed to evaluate a mixed target of car paint and soil. Blender 3D physics engines were used to create seven separate mixed target scenes. In each scene, a plane of blue car paint was covered with a different amount of soil contaminant. The bidirectional reflectance of each mixed target was calculated by DIRSIG within the solar plane (0° or 180° from solar azimuth), and perpendicular to the solar plane (90° or 270° from solar azimuth). The virtual hardware and illumination conditions described in Section 2.4 were used for this experiment. The relationship between reflectance and the amount of soil contamination was also observed for each car paint file. The fourteen different view locations from both the solar plane and the perpendicular plane were averaged to produce the reflectance percentage for each of the seven levels of soil contamination coverage. After all of these tests, the position of the solar source was changed (0° and 50° zenith) to evaluate the change in signal under new illumination conditions.

3. RESULTS

Goniometric simulations have been performed for a synthetic soil scene and the contamination scene described above. Soil scene results have been plotted with data from Wang[1] for direct comparison (Figure 3). BRDF percentage from the soil and contamination experiments are plotted in the principle and perpendicular plane orientations.

The soil simulation (Figure 4) displayed strong opposition effect backscatter in the solar plane with maximum reflectance values for red, green, and blue bands occurring at a zenith angle of 40° from nadir. All measurements taken at backscatter view angles had higher reflectance than data collected at forward scattering angles. This trend can be attributed to the surface roughness of the sample (Figure 5). The lack of a reflectance peak in the forward scattering plane indicates that geometric features of the target shadow and occlude one another. Data taken at larger declination angles is strongly influenced by this effect. In the perpendicular plane, peak reflectance occurred at nadir where the least amount of shadowing and occlusion will occur. This is also illustrated in Figure 5. Reflectance decreased uniformly as the view zenith angle increased in both the positive and negative direction. Simulated BRDF in the red, green and blue bands all vary from the measured lab data by an average of less than 6% of BRDF percentage, with standard deviations between 4% and 5%. There was 8% error of BRDF percentage in the blue band perpendicular plane measurements. All other measurements matched the measured data within a 6% error. The spectral contrast in both planes also says something about the geometry of the soil scene.

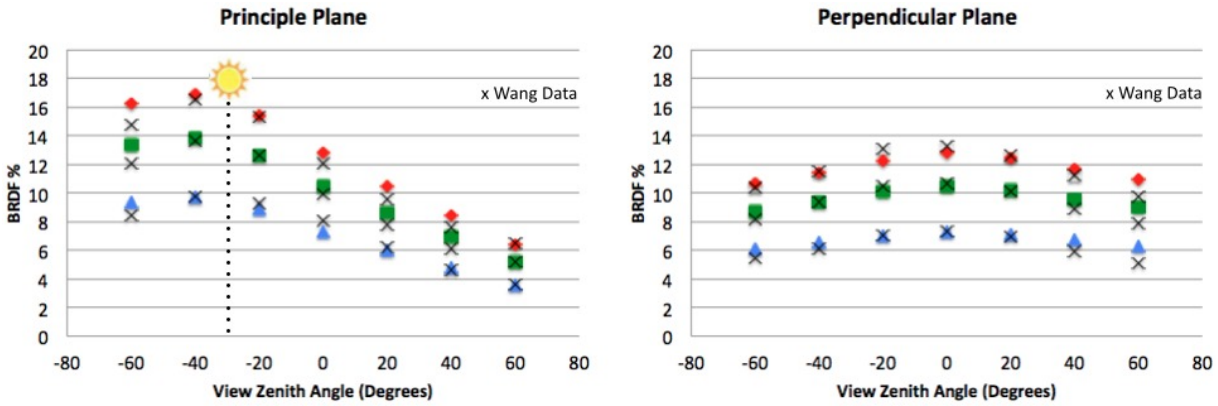

Figure 4. Soil BRDF% of DIRSIG generated R,G,B bands compared to the laboratory results of Wang[1]. Principle plane data is shown on the left while data collected perpendicular to the sun is shown on the right. The sun has a 30° zenith location.

The sensor geometry of forward and backscatter in the principle plane is defined in Figure 5. The most shadowing occurs in the forward scattering direction of the principle plane at large sensor declination angles. At these sensor locations, Figure 4 shows that the spectral contrast between red, green and blue bands is the smallest. This indicates that within shadows, there is little reflectance and that the true spectral nature of a sample will be masked. It is also observed that in the backscatter direction of the principle plane, spectral contrast is the highest. This sensor position is subjected to

the least amount of shadowing. In the perpendicular plane (Figure 4), spectral contrast remains relatively constant across all view zenith angles indicating that shadowing changes very little. When it does change, BRDF decreases in uniform fashion as the sensor zenith angle increases. This is expected for sensor positions in the perpendicular plane because the sensor does not detect the majority of forward and backscattered light. These trends are clearly visible in both the empirical and simulated results.

Figure 6 shows the contamination scene and the BRDF measurements made using NEFDS material files. Simulation predicts that the magnitude of blue band reflectance begins to dominate the green and red bands as more blue car paint is exposed. In the specular (forward scattering) direction, a lobe emerges as photons begin to interact with the intimate mixture of soil and car paint. This shows that within the same goniometric measurement, DIRSIG is simulating the red band dominant backscatter of light from soil and the directional specular reflection that is attributed to the blue car paint. It is apparent that the specular forward scatter becomes more definitive as the contaminant is removed from the metal car surface. As this occurs, contrast between the spectral bands is magnified when viewed in the forward specular direction.

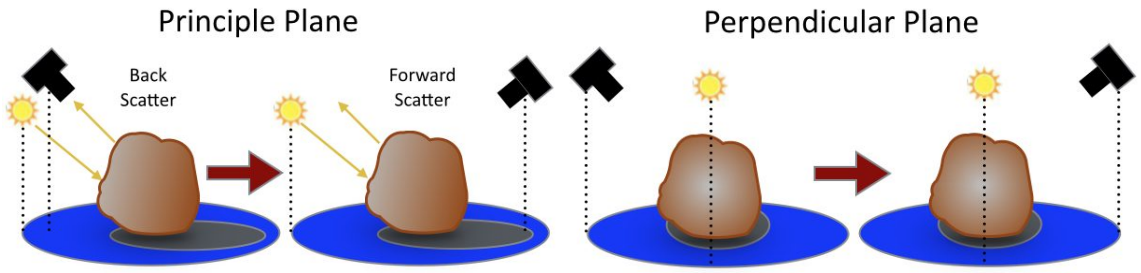

Figure 5. Principle plane measurements are made when a light source and a sensor have the same azimuth angle or when the source and sensor have azimuth angles that are 180° apart. A BRDF peak in the backscatter direction of the principle plane is observed in Figure 3. BRDF is noticeably smaller in the forward scatter direction of the principle plane because particle shadowing becomes prevalent. In the perpendicular plane, the least amount of shadowing and occlusion is observed when the sensor is directly above the target. Because the light source is located in a plane that is perpendicular to the sensor, the reflectance decreases uniformly as the sensor zenith angle is increased from the nadir position. Outside of the shadowed regions, the reflectance characteristics of the brown soil and blue car paint are clearly detected by sensors. Darkness dominates the shadowed regions of a target resulting in fewer reflected rays traveling between the target and the sensor. Reduced spectral contrast is the byproduct of these shadows. This is why the spectral contrast extremes occur in the backscatter and forward scattering directions.

After performing analysis on the contamination scenes with 30° illumination zenith, the study was extended to explore signature variations due to light source position. Additional data was collected for a target with 74% surface coverage and a source zenith angle of 50° (Figure 7). This BRDF data was then compared to a simulation with the same target illuminated at a 30° zenith angle. The change in source position revealed distinct BRDF features. In the principle plane, the backscatter hot spot was sensed at a zenith location 60° from nadir. Obeying the law of specular reflection, the forward scatter lobe also exhibited the same positional shift to larger zenith angles. The other significant characteristic of this geometry is that shadowing effects and backscatter are observed at zenith angles between nadir and 20°. This indicates that more occlusion is occurring in the 50° source zenith scene compared to the previously discussed scenario that had the light source positioned at a zenith angle of 30°. A reduction in BRDF magnitude is a consequence of the increasing levels of occlusion by the contaminating particles.

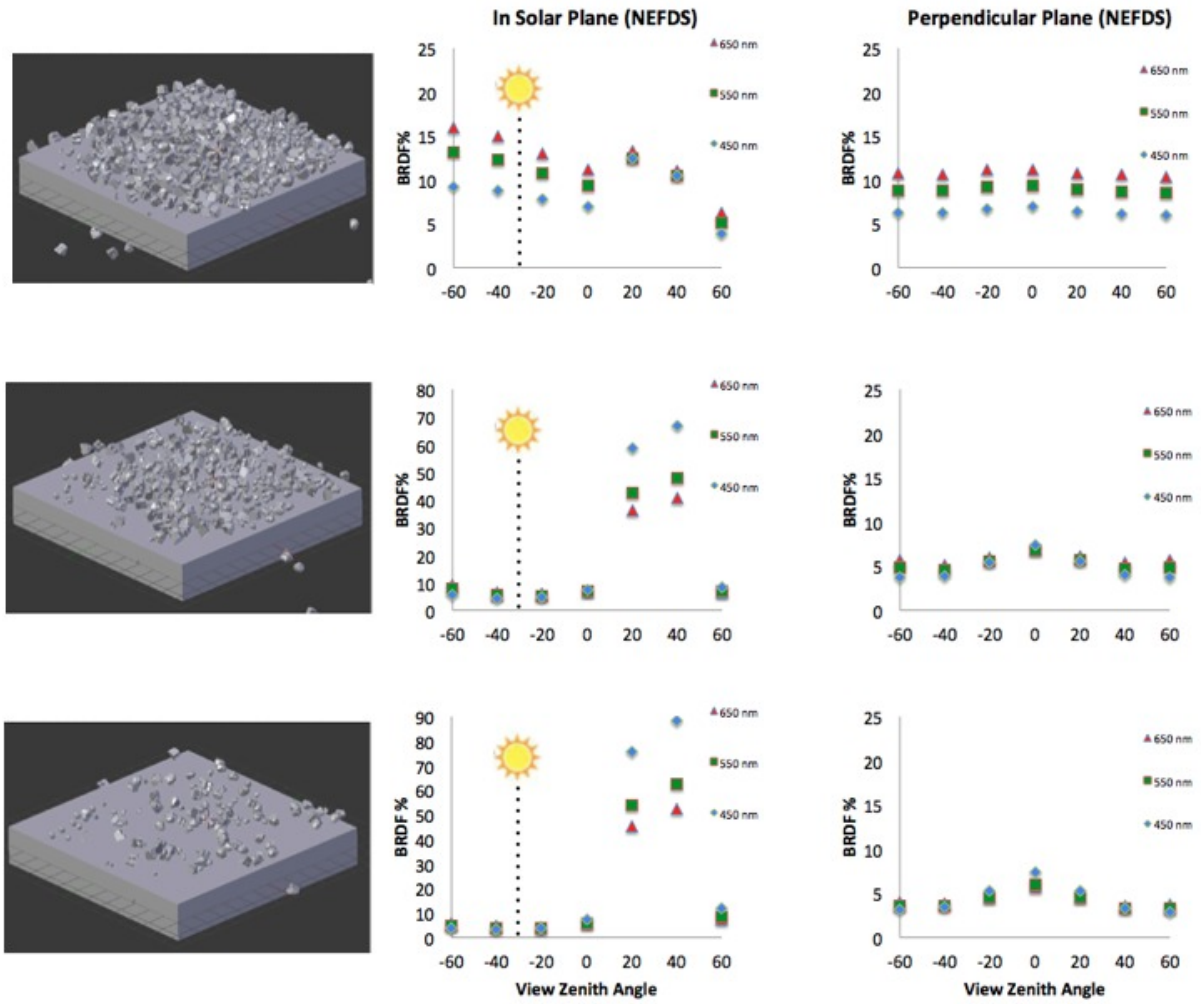

Figure 6. Simulated BRDF% is plotted for blue car paint contaminated with varying amounts of soil coverage. The target in the top plot is 90% covered with soil. The middle and bottom targets are 44% and 27% covered respectively. As surface coverage changes, BRDF and spectral contrast distinctions between targets becomes observable.

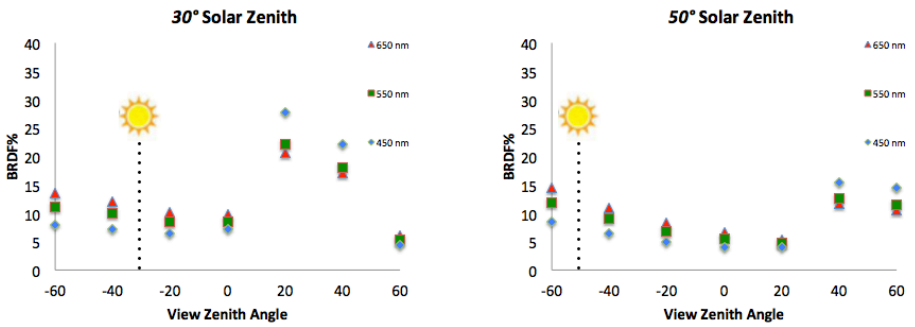

Figure 7. Simulations show the transformation in directional forward scatter as the source position changes between zenith angles of 30° and 50°.

Simulation was also used to describe how the magnitude of average reflectance changes with surface coverage (Figure 8). Data points from the principle and perpendicular planes were averaged together for each level of contamination coverage. Plots were formed for three light source positions (0°, 30° and 50° zenith). With the light source at nadir, it was seen that there is a linear relationship between average reflectance and surface coverage. Blue band reflection trends with a slightly negative slope while both red and green band reflection trend with a slightly positive slope. When the position of the source subtends a 30° zenith angle, all three bands maintain a linear pattern. However, each band trends with a negative slope. At a source zenith angle of 50°, all three bands show a nonlinear relationship between reflectance and surface coverage. This is due to shadowing and occlusion effects that disproportionately impact reflectance when sensor location is low in the sky. Also notice that average reflectance for the three bands is very similar when there is very little surface coverage, but there is noticeable spectral contrast when surface coverage approaches 100%. When there is little coverage, reflection is highly specular and most of the sensor viewing positions will detect very little radiance. And when the paint is entirely covered, prevalent diffuse reflectance causes radiance to be measured at most hemispherical view locations. So although there is a large difference in spectral contrast for clean car paint in the specular direction, there is little contrast in the average reflectance at large source declination angles. This causes the nonlinearity. It should be noted that data from each sensor location has also been evaluated individually with respect to surface coverage and source declination. The averaged curves shown in Figure 8 are dominated by view positions in the principle plane. In that plane, solar shadowing and particle occlusions are occur simultaneously. Even so, nonlinear-effects are more dramatic when the light source is low in the sky.

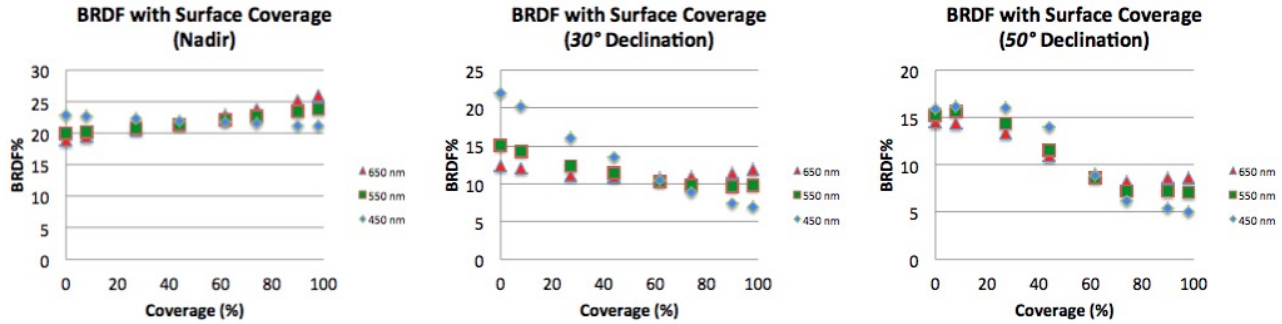

Figure 8. The simulated BRDF% with surface coverage was plotted for different solar positions. The linear and non-linear change in BRDF relate to solar zenith angle.

4. CONCLUSION

A virtual goniometer has been developed using DIRSIG and the NEFDS to model the directional scattering of light in the visible regime. A comparative experiment showed that this modeling technique accurately predicts spectral features of magnitude and contrast that are observed in laboratory measurements. Simulated soil BRDF varies from lab results by 4%-8% of BRDF percentage across red, green and blue spectral bands. The virtual goniometer framework was also used to predict spectral trends for dry soil contamination. Changes in solar position and surface coverage revealed significant trends in BRDF.

REFERENCES

[1] Wang, Z., C. A. Coburn, X. Ren, D. Mazumdar, S. Myshak, A. Mullin, and P. M. Teillet., "Assessment of soil surface BRDF using an imaging spectrometer." Proc. SPIE 7830, 7830101-7830109 (2010).
[2] Ben-Dor, E., S. Chabrillat, J. A. M. Demattê, G. R. Taylor, J. Hill, M. L. Whiting, and S. Sommer., "Using imaging spectroscopy to study soil properties." Remote Sensing of Environment 113, 38-55 (2009).
[3] Bachmann, C. M., W. Philpot, A. Abelev, and D. Korwan., "Phase angle dependence of sand density observable in hyperspectral reflectance." Remote Sensing of Environment 150, 53-65 (2014).

[4] Johnson, J. R., P. G. Lucey, K. A. Horton, and E. M. Winter., "Infrared measurements of pristine and disturbed soils 1. Spectral contrast differences between field and laboratory data." Remote Sensing of Environment 64, 34-46 (1998).
[5] Torrance, K. E., and E. M. Sparrow., "Theory for off-specular reflection from roughened surfaces." JOSA 57(9), 1105-1112 (1967).
[6] Westin, S. H., H. Li, and K. E. Torrance., "A comparison of four brdf models." Eurographics Symposium on Rendering. pags, 1-10 (2004).
[7] He, X. D., K. E. Torrance, F. X. Sillion, and D. P. Greenberg., "A comprehensive physical model for light reflection." ACM SIGGRAPH Computer Graphics 25(4), 175-186 (1991).
[8] Ngan, A., F. Durand, and W. Matusik., "Experimental Analysis of BRDF Models." Eurographics Symposium on Rendering 16, 117-126 (2005).
[9] Oren, M., and S. K. Nayar., "Generalization of the Lambertian model and implications for machine vision." International Journal of Computer Vision 14(3), 227-251 (1995).
[10] Hanrahan, P., and W. Krueger., "Reflection from layered surfaces due to subsurface scattering." ACM Conference on Computer graphics and interactive techniques 20, 165-174 (1993).
[11] Beckmann, P., and A. Spizzichino., [The scattering of electromagnetic waves from rough surfaces], Norwood, MA, Artech House, Inc., (1987).
[12] Ashikhmin, M., and P. Shirley., "An anisotropic phong BRDF model." Journal of graphics tools 5(2), 25-32 (2000).
[13] Hapke, B., [Theory of reflectance and emittance spectroscopy], Cambridge University Press, (2012).
[14] Gartley, M. G., J. R. Schott, and S. D. Brown., "Micro-scale modeling of contaminant effects on surface optical properties." Optical Engineering + Applications, 708601-708609 (2008)
[15] Schott, J. R., R. V. Raqueno, and C. Salvaggio., "Incorporation of a time-dependent thermodynamic model and a radiation propagation model into IR 3D synthetic image generation." Optical Engineering 31(7), 1505-1516 (1992).
[16] Schott, J. R., S. D. Brown, R. V. Raqueno, H. N. Gross, and G. Robinson., "An advanced synthetic image generation model and its application to multi/hyperspectral algorithm development." Canadian Journal of Remote Sensing 25(2), 99-111 (1999).
[17] Nicodemus, F.E., J.C. Richmond, and J.J Hsia, [Geometrical Considerations and Nomenclature for Reflectance], U.S. Department of Commerce, National Bureau of Standards, Washington, DC, (1977).
[18] B*ä*nninger, D., and H. Fl*ü*hler, "Modeling light scattering at soil surfaces." IEEE Transactions on Geoscience and Remote Sensing 42(7), 1462-1471 (2004).
[19] Li, Z. J., A. K. Fung, S. Tjuatja, D. P. Gibbs, C. L. Betty, and J. R. Irons, "A modeling study of backscattering from soil surfaces." IEEE Transactions on Geoscience and Remote Sensing 34(1), 264-271 (1996).
[20] Liang, S., and J. R. G. Townshend, "A modified Hapke model for soil bidirectional reflectance." Remote sensing of environment 55(1), 1-10 (1996).
[21] Kerekes, J. P., K. E. Strackerjan, and C. Salvaggio, "Spectral reflectance and emissivity of man-made surfaces contaminated with environmental effects." Optical Engineering 47(10), 106201 (2008).
[22] Maxwell, J. R., J. Beard, S. Weiner, D. Ladd, and S. Ladd [Bidirectional Reflectance Model Validation and Utilization.] Environmental Research Inst. of Michigan, Ann Arbor, MI, 196400-1-T, (1973).